# QUADRATURE AND SYMMETRY ON THE CUBED SPHERE

JEAN-BAPTISTE BELLET[†], MATTHIEU BRACHET[‡], AND JEAN-PIERRE CROISILLE[†]

Abstract. In the companion paper [J.-B. Bellet, M. Brachet & J.-P. Croisille, *Interpolation on the Cubed Sphere with Spherical Harmonics*, Preprint, 2021], a spherical harmonic subspace associated to the Cubed Sphere has been introduced. This subspace is further analyzed here. In particular, it permits to define a new Cubed Sphere based quadrature. This quadrature inherits the rotational invariance properties of the spherical harmonic subspace. Contrary to Gaussian quadrature, where the set of nodes and weights is solution of a nonlinear system, only the weights are unknown here. Despite this conceptual simplicity, the new quadrature displays an accuracy comparable to optimal quadratures, such as the Lebedev rules.

*Keywords: Quadrature rule on the sphere - Cubed Sphere Grid - Spherical Harmonics - Rotational invariance - Lebedev quadrature rule*

## 1. Introduction

We introduce a new quadrature rule defined on the equiangular Cubed Sphere grid.

Let $\mathrm{CS}_N \subset \mathbb{S}^2$ denote the Cubed Sphere with parameter $N$. In [6], a finite dimensional spherical harmonic subspace has been associated to the set of nodes $\mathrm{CS}_N$. This subspace, called $\mathcal{U}_N$ hereafter, provides existence and uniqueness to the Lagrange interpolation, with $\mathrm{CS}_N$ as set of nodes. Here our goal is to use the space $\mathcal{U}_N$ and the nodes of $\mathrm{CS}_N$ to define a new quadrature rule on the sphere $\mathbb{S}^2$.

The design of quadrature rules on the sphere can be classified as follows (see [13, Chap.40] and the references therein). In a first approach, one seeks a global system with the nodes and the weights as unknowns. Typical examples are the Lebedev rules [14] or the rule in [1]. In a second approach, the weights are supposed given and the nodes are unknown. This is the case in the theory of t-designs. We refer to [10] for a review. A third approach consists in imposing the set of nodes from the beginning and to have the weights as unknown. A particular case is the interpolatory approach, where the quadrature rule is obtained by integrating an interpolation polynomial. In this case, the choice of the nodes is crucial for the quality of the rule, [13, Chap.40, pp. 1200 sqq.]. In the present paper, we are in the latter case: we define a quadrature rule on $\mathrm{CS}_N$, by interpolation in the space $\mathcal{U}_N$ of spherical harmonics mentioned above.

Here the Cubed Sphere nodes are selected from the beginning as "good" quadrature nodes, and therefore, only the weights must be identified. In [16], two examples of weights have been suggested. The first one was based on some extended trapezoidal rule, attributing some area to each node. The second one was defined as a perturbation of the first one with a design based on some optimization principle. See also [7] for another rule, including a Simpson like formula. Here we come back to the general question of the "best choice" of weights associated to the Cubed Sphere nodes. As in the general approach, we require exactness of the quadrature for a particular set of spherical harmonics. Using the space $\mathcal{U}_N$ in [6] immediately delivers a quadrature rule. This quadrature is different from the ones mentioned above. The space $\mathcal{U}_N$ remarkably enjoys invariance under the action of the group of the cube. This is somehow expected, since the group of $\mathrm{CS}_N$ is in fact the group of the cube, (or of the octahedron) [5]. As will be shown below, the new quadrature rule inherits this invariance. This property is highly desirable. It is well known that group invariance is the backbone for the design of highly accurate spherical quadratures, [1, 14, 15, 18].

*Date*: January 23, 2022.

2010 *Mathematics Subject Classification.* 65D05, 65D30, 65D32.

*Key words and phrases.* Cubed sphere, interpolation, quadrature, octahedral group.

The paper is organized as follows. Section 2 gives the notation on the spherical harmonics, the Cubed Sphere and its group. Section 3 recalls how the space $\mathcal{U}_N$ is defined and Section 4 establishes several of its invariance properties. In Section 5, the new quadrature is introduced. By construction, this quadrature is exact on the space $\mathcal{U}_N$. In addition, it is invariant under the octahedral group. This implies that it is exact for a proportion of 15/16 of all (real) Legendre spherical harmonics. Finally in Section 6, we display numerical results for a large series of test cases. It is observed that the new rule is only slightly suboptimal, when compared to the optimal Lebedev rules. This somehow supports the main Ansatz of this study, namely that the Cubed Sphere nodes are good quadrature nodes on the sphere. [1]

## 2. Background and notation

The real Legendre spherical harmonics of degree $n$ are normalized as follows:

$$Y_n^m(x) = Y_n^m(\theta,\phi) = (-1)^{|m|}\sqrt{\tfrac{(n+1/2)(n-|m|)!}{\pi(n+|m|)!}}P_n^{|m|}(\sin\theta)\times\begin{cases}\sin|m|\phi, & m<0,\\ \frac{1}{\sqrt{2}}, & m=0,\\ \cos m\phi, & m>0.\end{cases}$$

Here, $P_n^{|m|}(t) = (-1)^{|m|}(1-t^2)^{|m|/2}\frac{\mathrm{d}^{|m|+n}}{\mathrm{d}t^{|m|+n}}\frac{1}{2^n n!}(t^2-1)^n$ is the associated Legendre function, and we set $x = (\cos\theta\cos\phi, \cos\theta\sin\phi, \sin\theta)$ with $(\theta,\phi)\in[-\frac{\pi}{2},\frac{\pi}{2}]\times[-\pi,\pi]$, the latitude/longitude angles. The family $(Y_n^m)_{-n\le m\le n}$ is an orthonormal basis of the subspace $\mathcal{Y}_n\subset L^2(\mathbb{S}^2)$, for the inner product

$$\langle u,v\rangle_{L^2(\mathbb{S}^2)} = \int_{\mathbb{S}^2} u(x)v(x)\mathrm{d}\sigma.$$

The infinite family $(Y_n^m)_{|m|\le n, n\in\mathbb{N}}$ is a Hilbert basis of $L^2(\mathbb{S}^2)$.

The equiangular Cubed Sphere $\mathrm{CS}_N\subset\mathbb{S}^2$, is defined by

$$\mathrm{CS}_N := \Big\{\tfrac{1}{\sqrt{1+u^2+v^2}}(\pm1,u,v),\ \tfrac{1}{\sqrt{1+u^2+v^2}}(u,\pm1,v),\ \tfrac{1}{\sqrt{1+u^2+v^2}}(u,v,\pm1);\\ u=\tan\tfrac{i\pi}{2N}, v=\tan\tfrac{j\pi}{2N}, -\tfrac{N}{2}\le i,j\le\tfrac{N}{2}\Big\}.$$

For ease of notation, we denote the nodes of $\mathrm{CS}_N$ by $x_i$, $1\le i\le\bar{N}$, where $\bar{N}=6N^2+2$ is the cardinal number:

$$\mathrm{CS}_N = \{x_i,\ 1\le i\le\bar{N}\}.$$

The symmetry group of the Cubed Sphere is given in the following theorem [5].

**Theorem 1** (Symmetry group of the Cubed Sphere)**.** *An orthogonal matrix $Q$ leaves the Cubed Sphere $\mathrm{CS}_N$ invariant if, and only if, it leaves the octahedron*

$$\{(\pm1,0,0),(0,\pm1,0),(0,0,\pm1)\}$$

*invariant. In other words, the symmetry group $\mathcal{G}$ of $\mathrm{CS}_N$ is exactly the full octahedral group. Its matrix representation is given by*

$$\mathcal{G} = \left\{\begin{bmatrix}\epsilon_1 e_{\sigma_1} & \epsilon_2 e_{\sigma_2} & \epsilon_3 e_{\sigma_3}\end{bmatrix}, \sigma\in\mathfrak{S}_3, \epsilon\in\{-1,1\}^3\right\},\quad \textit{with}\quad e_1=(1,0,0),\ e_2=(0,1,0),\ e_3=(0,0,1).$$

The space of real functions defined on $\mathrm{CS}_N$ is denoted by

$$\mathcal{F}(\mathrm{CS}_N) = \{f:\mathrm{CS}_N\to\mathbb{R}\}.$$

The canonical basis $(\delta_{x_i})_{1\le i\le\bar{N}}$ of $\mathcal{F}(\mathrm{CS}_N)$ is defined by

$$\delta_{x_i}(x_j) = \delta_{ij} = \begin{cases}1, & \text{if } i=j,\\ 0, & \text{otherwise,}\end{cases}\qquad 1\le i,j\le\bar{N}.$$

[1] Appendix A reports URLs with some available quadrature rules. In particular, the new rule $\mathcal{Q}_N$ data are available in an open archiv.

In this basis, any $f \in \mathcal{F}(\mathrm{CS}_N)$ is represented by the column vector $[f(x_i)]_{1\leq i\leq \bar{N}} \in \mathbb{R}^{\bar{N}}$, due to the decomposition

$$f = \sum_{i=1}^{\bar{N}} f(x_i)\delta_{x_i}.$$

For any real function defined on the sphere, $u : x \in \mathbb{S}^2 \mapsto u(x) \in \mathbb{R}$, the restriction of $u$ on $\mathrm{CS}_N$ is the function defined by

$$u|_{\mathrm{CS}_N} := \sum_{i=1}^{\bar{N}} u(x_i)\delta_{x_i} \in \mathcal{F}(\mathrm{CS}_N), \quad u|_{\mathrm{CS}_N}(x_i) = u(x_i),\ 1 \leq i \leq \bar{N}. \tag{1}$$

## 3. Interpolation on the Cubed Sphere with spherical harmonics

In [6], we have introduced a subspace $\mathcal{U}_N$ of real spherical harmonics, dedicated to Lagrange interpolation on the Cubed Sphere $\mathrm{CS}_N$. Our presentation here is deduced from intrinsic properties of $\mathcal{U}_N$ proved in [6][2].

First, we introduce a subspace $\mathcal{W}_n$ of spherical harmonics of degree $n$, defined by

$$\mathcal{W}_0 := \{0\}, \quad \mathcal{W}_n := \{u \in \mathcal{Y}_n : \exists v \in \mathcal{Y}_0 \oplus \cdots \oplus \mathcal{Y}_{n-1}, u|_{\mathrm{CS}_N} = v|_{\mathrm{CS}_N}\},\ n \geq 1. \tag{2}$$

Intuitively, $\mathcal{W}_n$ contains spherical harmonics of degree $n$ which are undersampled on $\mathrm{CS}_N$. Second, we build an orthogonal decomposition based on this subspace,

$$\mathcal{Y}_n = \mathcal{V}_n \oplus \mathcal{W}_n, \quad \text{with} \quad \mathcal{V}_n := (\mathcal{W}_n)^{\perp_{\mathcal{Y}_n}} = \{u \in \mathcal{Y}_n : \forall v \in \mathcal{W}_n, \langle u, v\rangle_{L^2(\mathbb{S}^2)} = 0\}. \tag{3}$$

In the orthogonal complement $\mathcal{V}_n$, any spherical harmonics can be reconstructed by interpolation on $\mathrm{CS}_N$ (unlike $\mathcal{W}_n$). This claim is part of the following theorem [6].

**Theorem 2.** *There exists an integer $N'$ such that the Lagrange interpolation problem has always a unique solution in $\mathcal{V}_0 \oplus \cdots \oplus \mathcal{V}_{N'}$,* i.e.

$$\forall f \in \mathcal{F}(\mathrm{CS}_N), \quad \exists! u \in \mathcal{V}_0 \oplus \cdots \oplus \mathcal{V}_{N'}, \quad u|_{\mathrm{CS}_N} = f, \quad (\text{i.e., } \forall 1 \leq j \leq \bar{N},\ u(x_j) = f(x_j)). \tag{4}$$

This theorem justifies the following definition.

**Definition 3** (Interpolation space)**.** Let $\mathcal{V}_n$ denote the orthogonal complement (3) of the *undersampled subspace* $\mathcal{W}_n$, defined by (2). The *interpolation space* on $\mathrm{CS}_N$ is defined as

$$\mathcal{U}_N := \mathcal{V}_0 \oplus \cdots \oplus \mathcal{V}_{N'}, \tag{5}$$

where $N' \geq 0$ is the smallest integer such that (4) is realized.

We refer to [6] for a practical algorithm to compute a real orthonormal basis of $\mathcal{U}_N$, denoted here by $(u_j)_{1\leq j\leq \bar{N}}$. Then,

$$u_j \in \mathcal{U}_N, \quad \langle u_i, u_j\rangle_{L^2(\mathbb{S}^2)} = \delta_{ij}, \quad 1 \leq i, j \leq \bar{N}.$$

Without loss of generality, the first basis function is $u_1(x) = \frac{1}{\sqrt{4\pi}} \in \mathcal{Y}_0$. By definition of $\mathcal{U}_N$, the following linear map is isomorphic:

$$\begin{array}{rccc} T_N : & \mathcal{U}_N & \longrightarrow & \mathcal{F}(\mathrm{CS}_N) \\ & u & \longmapsto & u|_{\mathrm{CS}_N}. \end{array}$$

The matrix of $T_N$, in the canonical basis $(\delta_{x_i})_{1\leq i\leq \bar{N}}$ of $\mathcal{F}(\mathrm{CS}_N)$, and the basis $(u_j)_{1\leq j\leq \bar{N}}$ of $\mathcal{U}_N$, is the *Vandermonde matrix* given by

$$A = [u_j(x_i)]_{1\leq i,j\leq \bar{N}}, \tag{6}$$

where $i$ is the row index, and $j$ is the column index. In (4), the solution $u \in \mathcal{U}_N$ is given by $u = T_N^{-1} f \in \mathcal{U}_N$. This suggests to define an *interpolation operator*, by $\mathcal{I}_N := T_N^{-1}$. Then, the unique element of $\mathcal{U}_N$ interpolating $f \in \mathcal{F}(\mathrm{CS}_N)$ is given by $\mathcal{I}_N f \in \mathcal{U}_N$, and is represented by the column vector $A^{-1}[f(x_i)] \in \mathbb{R}^{\bar{N}}$,

$$\mathcal{I}_N f(x) = [u_j(x)]A^{-1}[f(x_i)], \quad x \in \mathbb{S}^2.$$

[2]The space $\mathcal{U}_N$ was denoted by $\mathcal{Y}'_{N'}$ in [6].

## 4. Rotational invariance of the interpolation space

In this section, we study the invariance of the interpolation space $\mathcal{U}_N$ under the symmetry group $\mathcal{G}$ of the Cubed Sphere. We call "rotated" a function defined as follows.

**Definition 4** ("Rotated" function)**.** Assume that $Q \in \mathcal{G}$ leaves a set $E$ invariant, *i.e.* $Q^\intercal E = E$. Let $f : E \to \mathbb{R}$ be a function defined on $E$. The "rotated" function, denoted by $f(Q^\intercal \cdot)$, is the function

$$f(Q^\intercal \cdot) : x \in E \mapsto f(Q^\intercal x) \in \mathbb{R}.$$

Our main invariance result is the following theorem.

**Theorem 5** (Invariance of the interpolation space)**.** *Let $n \geq 0$.*
*(i) The undersampled subspace $\mathcal{W}_n$ is invariant under $\mathcal{G}$,* i.e.

$$\forall Q \in \mathcal{G},\ \forall u \in \mathcal{W}_n,\ u(Q^\intercal \cdot) \in \mathcal{W}_n.$$

*(ii) The subspace $\mathcal{V}_n = \mathcal{W}_n^\perp$ is invariant under $\mathcal{G}$,* i.e.

$$\forall Q \in \mathcal{G},\ \forall u \in \mathcal{V}_n,\ u(Q^\intercal \cdot) \in \mathcal{V}_n.$$

*(iii) The interpolation space $\mathcal{U}_N$ is invariant under $\mathcal{G}$,* i.e.

$$\forall Q \in \mathcal{G},\ \forall u \in \mathcal{U}_N,\ u(Q^\intercal \cdot) \in \mathcal{U}_N.$$

*Proof.* Fix $Q \in \mathcal{G}$, *i.e.* $Q \in \mathbb{R}^{3\times 3}$ is an orthogonal matrix such that $Q^\intercal \mathrm{CS}_N = \mathrm{CS}_N$.
(i) If $n = 0$, $\mathcal{W}_0 = \{0\}$ is invariant under $\mathcal{G}$. Fix now $u \in \mathcal{W}_n \subset \mathcal{Y}_n$ with $n \geq 1$. There exists $v \in \mathcal{Y}_0 \oplus \cdots \oplus \mathcal{Y}_{n-1}$ such that $u|_{\mathrm{CS}_N} = v|_{\mathrm{CS}_N}$, or equivalently, $(u-v)|_{\mathrm{CS}_N} = 0$. Firstly, $u(Q^\intercal \cdot) \in \mathcal{Y}_n$ and $v(Q^\intercal \cdot) \in \mathcal{Y}_0 \oplus \cdots \oplus \mathcal{Y}_{n-1}$. Secondly, $(u(Q^\intercal \cdot) - v(Q^\intercal \cdot))\,|_{\mathrm{CS}_N} = (u-v)|_{\mathrm{CS}_N}(Q^\intercal \cdot) = 0$, and therefore $u(Q^\intercal \cdot)|_{\mathrm{CS}_N} = v(Q^\intercal \cdot)|_{\mathrm{CS}_N}$; here, the commutation between rotation and restriction is justified by the following lemma.

**Lemma 6** (Rotation commutes with restriction)**.** *For all $Q \in \mathcal{G}$, $n \geq 0$, and $u \in \mathcal{Y}_0 \oplus \cdots \oplus \mathcal{Y}_n$,*

$$u(Q^\intercal \cdot)|_{\mathrm{CS}_N} = u|_{\mathrm{CS}_N}(Q^\intercal \cdot) \in \mathcal{F}(\mathrm{CS}_N).$$

We postpone the proof of the lemma until the end of this section.
(ii) The result is a combination of (i) and $\mathcal{V}_n = \mathcal{W}_n^\perp$. Indeed, fix $u \in \mathcal{V}_n \subset \mathcal{Y}_n$ with $n \geq 0$. Then $u(Q^\intercal \cdot) \in \mathcal{Y}_n$. Furthermore, for every $v \in \mathcal{W}_n$,

$$\langle u(Q^\intercal \cdot), v\rangle_{L^2(\mathbb{S}^2)} = \int_{\mathbb{S}^2} u(Q^\intercal x)v(x)\mathrm{d}\sigma = \int_{\mathbb{S}^2} u(y)v(Qy)\mathrm{d}\sigma = \langle u, v(Q\cdot)\rangle_{L^2(\mathbb{S}^2)}\,; \quad (y := Q^\intercal x).$$

$\mathcal{W}_n$ is invariant under $\mathcal{G}$, so $v(Q\cdot) \in \mathcal{W}_n$. Then $v(Q\cdot)$ is orthogonal to $u$ since $u \in \mathcal{W}_n^\perp$. Therefore $\langle u(Q^\intercal \cdot), v\rangle = \langle u, v(Q\cdot)\rangle = 0$, which proves that $u(Q^\intercal \cdot) \in \mathcal{W}_n^\perp$.
(iii) The space $\mathcal{U}_N = \mathcal{V}_0 \oplus \cdots \oplus \mathcal{V}_{N'}$ is a sum of invariant subspaces due to (ii). □

**Corollary 7** (Interpolation and symmetry)**.** *(i) The interpolation operator commutes with any symmetry of the group $\mathcal{G}$:*

$$\forall f \in \mathcal{F}(\mathrm{CS}_N),\ \forall Q \in \mathcal{G},\ [\mathcal{I}_N f](Q^\intercal \cdot) = \mathcal{I}_N[f(Q^\intercal \cdot)].$$

*(ii) The interpolation operator preserves the invariance property; in other words, if $f \in \mathcal{F}(\mathrm{CS}_N)$ is invariant under $\mathcal{G}$,* i.e. $\forall Q \in \mathcal{G}$, $f(Q^\intercal \cdot) = f$, *then $\mathcal{I}_N f$ is invariant under $\mathcal{G}$,* i.e. $\forall Q \in \mathcal{G}$, $[\mathcal{I}_N f](Q^\intercal \cdot) = \mathcal{I}_N f$.

*Proof.* (i) Firstly, $f(Q^\intercal \cdot) \in \mathcal{F}(\mathrm{CS}_N)$ and $u = \mathcal{I}_N[f(Q^\intercal \cdot)] \in \mathcal{U}_N$ is the unique element of $\mathcal{U}_N$ such that $u|_{\mathrm{CS}_N} = f(Q^\intercal \cdot)$. Secondly, $v = \mathcal{I}_N f \in \mathcal{U}_N$ is the unique element of $\mathcal{U}_N$ such that $v|_{\mathrm{CS}_N} = f$. Due to Theorem 5.(iii), $v(Q^\intercal \cdot) \in \mathcal{U}_N$. By Lemma 6, $v(Q^\intercal \cdot)|_{\mathrm{CS}_N} = v|_{\mathrm{CS}_N}(Q^\intercal \cdot) = f(Q^\intercal \cdot)$, which proves $u = v(Q^\intercal \cdot)$. (ii) is an immediate consequence of (i). □

*Proof of Lemma 6.* Firstly, $\mathcal{Y}_0 \oplus \cdots \oplus \mathcal{Y}_n$ is invariant under the action of $Q$. Therefore $[u(Q^\intercal \cdot) : x \in \mathbb{S}^2 \mapsto u(Q^\intercal x)] \in \mathcal{Y}_0 \oplus \cdots \oplus \mathcal{Y}_n$, and $u(Q^\intercal \cdot)|_{\mathrm{CS}_N}$ is defined by

$$u(Q^\intercal \cdot)|_{\mathrm{CS}_N} = \sum_{i=1}^{\bar{N}} u(Q^\intercal x_i)\delta_{x_i} \in \mathcal{F}(\mathrm{CS}_N).$$

On the other hand, $[u|_{\mathrm{CS}_N} : x \in \mathrm{CS}_N \mapsto u(x)] \in \mathcal{F}(\mathrm{CS}_N)$, with $\mathrm{CS}_N$ left invariant by $Q$. Then the function $u|_{\mathrm{CS}_N}(Q^\intercal \cdot)$ is well-defined and is given by

$$u|_{\mathrm{CS}_N}(Q^\intercal \cdot) : x \in \mathrm{CS}_N \mapsto u(Q^\intercal x) \in \mathcal{F}(\mathrm{CS}_N).$$

At every $x = x_i \in \mathrm{CS}_N$, the two functions have the same value, $u(Q^\intercal x_i)$. □

## 5. A new quadrature on the Cubed Sphere

In this section, we introduce a new quadrature rule on $\mathrm{CS}_N$; it is defined by interpolation as follows.

**Theorem 8** (Quadrature rule)**.** *Let $u : \mathbb{S}^2 \to \mathbb{R}$ be a given function. The quadrature rule $\mathcal{Q}_N$ is defined by*

$$\mathcal{Q}_N u := \int_{\mathbb{S}^2} \mathcal{I}_N[u|_{\mathrm{CS}_N}](x)\mathrm{d}\sigma.$$

*(i) The formula $\mathcal{Q}_N$ can be expressed as follows:*

$$\mathcal{Q}_N u = \sum_{j=1}^{\bar{N}} \omega_N(x_j) u(x_j), \tag{7}$$

*where the weight function $\omega_N \in \mathcal{F}(\mathrm{CS}_N)$ is defined by*

$$[\omega_N(x_j)] = (A^\intercal)^{-1}[\sqrt{4\pi}\ 0\ \cdots\ 0]^\intercal, \tag{8}$$

*with $A$ the Vandermonde matrix* (6)*.*
*(ii) The formula $\mathcal{Q}_N$ is exact on the space $\mathcal{U}_N$ in (5),* i.e.

$$\forall u \in \mathcal{U}_N, \quad \mathcal{Q}_N u = \int_{\mathbb{S}^2} u(x)\mathrm{d}\sigma.$$

*(iii) The rule $\mathcal{Q}_N$ and the weight function $\omega_N$ is invariant under the group $\mathcal{G}$ of* $\mathrm{CS}_N$*,* i.e.

$$\forall Q \in \mathcal{G}, \quad \forall u \in \mathcal{U}_N,\ \mathcal{Q}_N(u(Q^\intercal \cdot)) = \mathcal{Q}_N(u), \quad \textit{and} \quad \omega_N(Q^\intercal \cdot) = \omega_N.$$

*Proof.* (i-ii) Firstly, if $u \in \mathcal{U}_N$, $\mathcal{Q}_N$ exactly integrates $u$, since $u$ coincides with $\mathcal{I}_N u$. In particular, for each basis function $u_j \in \mathcal{U}_N$, $\mathcal{Q}_N u_j = \int_{\mathbb{S}^2} u_j(x)\mathrm{d}\sigma$. For $u_1 = \frac{1}{\sqrt{4\pi}}$, $\int_{\mathbb{S}^2} u_1(x)\mathrm{d}\sigma = \sqrt{4\pi}$. For every $1 \le j \le \bar{N}$, $u_j \perp u_1$, which means $\int_{\mathbb{S}^2} u_j(x)\mathrm{d}\sigma = 0$. Then, $[\mathcal{Q}_N u_j]_{1\le j\le \bar{N}} = [\sqrt{4\pi}\ 0\ \cdots\ 0]^\intercal$. Secondly, define $\omega_N \in \mathcal{F}(\mathrm{CS}_N)$ by

$$\omega_N(x_i) = \int_{\mathbb{S}^2} \mathcal{I}_N[\delta_{x_i}]\mathrm{d}\sigma, \quad 1 \le i \le \bar{N}. \tag{9}$$

By linearity, we deduce from (1) that

$$\mathcal{Q}_N u = \sum_{i=1}^{\bar{N}} \omega_N(x_i) u(x_i) = [u(x_i)]^\intercal [\omega_N(x_i)].$$

Using the basis functions, we obtain

$$A^\intercal [\omega_N(x_i)]_{1\le i\le \bar{N}} = [\mathcal{Q}_N u_j]_{1\le j\le \bar{N}} = [\sqrt{4\pi}\ 0\ \cdots\ 0]^\intercal,$$

This gives (8) using the fact that the matrix $A^\intercal \in \mathbb{R}^{\bar{N}\times\bar{N}}$ is non singular.

*Remark* 9. In [6], a LQ-factorization of $A^\intercal$ is computed, $A^\intercal = LQ$ where $L$ is lower triangular and $Q$ is orthogonal. Thus, the weight function $\omega_N$ is calculated from a linear system with matrix $L$ as $[\omega_N(x_j)] = Q^\intercal L^{-1}[\sqrt{4\pi}\ 0\ \cdots\ 0]^\intercal$.

(iii) Fix $Q \in \mathcal{G}$ and $u \in \mathcal{U}_N$. By Theorem 5, $u(Q^\intercal \cdot) \in \mathcal{U}_N$. Thus, using (ii) and a change of variable yields

$$\mathcal{Q}_N(u(Q^\intercal \cdot)) = \int_{\mathbb{S}^2} u(Q^\intercal x)\mathrm{d}\sigma = \int_{\mathbb{S}^2} u(x)\mathrm{d}\sigma = \mathcal{Q}_N(u).$$

Fix now $1 \leq i \leq \bar{N}$ and denote $u = \mathcal{I}_N \delta_{x_i} \in \mathcal{U}_N$. By Corollary 7, $u(Q^\intercal \cdot) = \mathcal{I}_N[\delta_{x_i}(Q^\intercal \cdot)] \in \mathcal{U}_N$, with $\delta_{x_i}(Q^\intercal \cdot) = \delta_{Qx_i}$. Therefore by (9), $\mathcal{Q}_N(u) = \omega_N(x_i)$ and $\mathcal{Q}_N(u(Q^\intercal \cdot)) = \omega_N(Qx_i)$. Then, by invariance of $\mathcal{Q}_N$,

$$\omega_N(x_i) = \mathcal{Q}_N(u) = \mathcal{Q}_N(u(Q^\intercal \cdot)) = \omega_N(Qx_i). \qquad \square$$

According to Theorem 8 (ii), the quadrature rule $\mathcal{Q}_N$ exactly integrates the $\bar{N}$ spherical harmonics of $\mathcal{U}_N$. Taking benefit from the rotational invariance, we prove furthermore that it exactly integrates an infinite number of spherical harmonics.

**Corollary 10.** *The quadrature rule $\mathcal{Q}_N$ exactly integrates a ratio of $\frac{15}{16}$ of **all** real Legendre spherical harmonics. More precisely, for all $|m| \leq n$,*

$$\mathcal{Q}_N(Y_n^m) = \int_{\mathbb{S}^2} Y_n^m(x)\mathrm{d}\sigma, \quad \textit{if} \quad \begin{cases} n \equiv 1\,(2), \\ \textit{or, } m < 0, \\ \textit{or, } m \geq 0 \textit{ and } m \equiv 1, 2, 3\,(4); \end{cases}$$

*equivalently, $\mathcal{Q}_N(Y_n^m) \neq \int_{\mathbb{S}^2} Y_n^m(x)\mathrm{d}\sigma \Rightarrow n \equiv 0\,(2)$, $m \geq 0$ and $m \equiv 0\,(4)$.*

*Proof.* Fix $n \geq 1$ and $|m| \leq n$. Then $\int_{\mathbb{S}^2} Y_n^m(x)\mathrm{d}\sigma = 0$. For well chosen integers $n$, $m$, we build a symmetry $Q \in \mathcal{G}$ such that $Y_n^m(Q^\intercal \cdot) = -Y_n^m$. This will imply $\mathcal{Q}_N(Y_n^m) = \mathcal{Q}_N(Y_n^m(Q^\intercal \cdot)) = -\mathcal{Q}_N(Y_n^m)$, which proves $\mathcal{Q}_N(Y_n^m) = 0 = \int_{\mathbb{S}^2} Y_n^m(x)\mathrm{d}\sigma$. In the spherical coordinate system $x(\theta, \phi) = (\cos\theta\cos\phi, \cos\theta\sin\phi, \sin\theta)$, $\phi \in [-\pi, \pi]$, $\theta \in [-\frac{\pi}{2}, \frac{\pi}{2}]$, we denote $Y_n^m(x(\theta, \phi)) := Y_n^m(\theta, \phi)$.

*Case 1: $n \equiv 1\,(2)$ and $m \equiv 0\,(4)$.* Then $\theta \mapsto P_n^{|m|}(\sin\theta)$ is odd, so is $\theta \mapsto Y_n^m(x(\theta, \phi))$; hence,

$$Y_n^m(Q^\intercal x(\theta, \phi)) = Y_n^m(x(-\theta, \phi)) = -Y_n^m(x(\theta, \phi)), \quad \text{for} \quad Q := \begin{bmatrix} 1 & 0 & 0 \\ 0 & 1 & 0 \\ 0 & 0 & -1 \end{bmatrix}.$$

*Case 2: $m < 0$.* Then $\phi \mapsto Y_n^m(x(\theta, \phi))$ is odd, so,

$$Y_n^m(Q^\intercal x(\theta, \phi)) = Y_n^m(x(\theta, -\phi)) = -Y_n^m(x(\theta, \phi)), \quad \text{for} \quad Q := \begin{bmatrix} 1 & 0 & 0 \\ 0 & -1 & 0 \\ 0 & 0 & 1 \end{bmatrix}.$$

*Case 3: $m \equiv 1, 3\,(4)$.* Then $m(\phi + \pi) \equiv m\phi + \pi\,(2\pi)$, and

$$Y_n^m(Q^\intercal x(\theta, \phi)) = Y_n^m(x(\theta, \phi + \pi)) = -Y_n^m(x(\theta, \phi)), \quad \text{for} \quad Q := \begin{bmatrix} -1 & 0 & 0 \\ 0 & -1 & 0 \\ 0 & 0 & 1 \end{bmatrix}.$$

*Case 4: $m \equiv 2\,(4)$.* Then $m(\phi + \frac{\pi}{2}) \equiv m\phi + \pi\,(2\pi)$, and

$$Y_n^m(Q^\intercal x(\theta, \phi)) = Y_n^m(x(\theta, \phi + \tfrac{\pi}{2})) = -Y_n^m(x(\theta, \phi)), \quad \text{for} \quad Q := \begin{bmatrix} 0 & 1 & 0 \\ -1 & 0 & 0 \\ 0 & 0 & 1 \end{bmatrix}. \qquad \square$$

*Remark* 11. In Corollary 10 (and its proof), the quadrature rule $\mathcal{Q}_N$ can be replaced by any linear form $\mathcal{Q} : L^2(\mathbb{S}^2) \to \mathbb{R}$ which is invariant under the octahedral group $\mathcal{G}$. In particular, the 15/16-property of the corollary holds for any spherical quadrature with octahedral symmetry. Therefore Corollary 10 also holds for the Lebedev rules [14].

*Remark* 12. The ratio "15/16" of the real Legendre basis is obtained asymptotically. In [7, 16], a similar approach based on invariance properties reported an asymptotic ratio of 7/8 of the complex Legendre basis exactly integrated. Here, in the proof of Corollary 10, the real Legendre basis is used instead. Using this basis allows to prove that exact quadrature actually holds up to the ratio of 15/16 of all spherical harmonics.

## 6. Numerical results

6.1. **Symmetry invariance assessment.** We begin by two numerical assessments related to interpolation in $\mathcal{U}_N$.

First, we illustrate that the interpolation operator $\mathcal{I}_N$ preserves the invariance property, as stated in Corollary 7.(ii). Fix $N = 6$ and consider the series of symmetric functions $g_i \in \mathcal{F}(\mathrm{CS}_N)$, described in Table 1. By construction, each function $g_i$, $1 \leq i \leq 6$, is constant along any orbit, *i.e.* $\forall Q \in \mathcal{G}$, $g_i(Q^\intercal \cdot) = g_i$, and is supported by a set of symmetric nodes. For $i \leq 5$, $g_i$ takes the value 1 along the orbit of $a_i \in \mathrm{CS}_N$, and the value 0 otherwise. The orbit of $a_1$ contains the vertices of an octahedron. The orbit of $a_2$ contains the vertices of a cube. The orbit of $a_3$ contains the vertices of a cubaoctahedron. The orbit of $a_4$ is included in the edges of an octahedron. The orbit of $a_5$ is "generic", with cardinal number 48. The Figure 1 displays how the symmetry is reflected in the interpolating functions $\mathcal{I}_N g_i \in \mathcal{U}_N$, $1 \leq i \leq 6$. The octahedral symmetry predicted by Corollary 7.(ii) can be observed; the functions $\mathcal{I}_N g_i$ are constant along any orbit.

| $i$ | $g_i$ | $a_i$ | $\lvert \operatorname{supp} g_i \rvert$ |
|---|---|---|---|
| 1 | $\frac{1}{8}\sum_{Q\in\mathcal{G}} \delta_{Qa_1}$ | $[1\,0\,0]^\intercal$ | 6 |
| 2 | $\frac{1}{6}\sum_{Q\in\mathcal{G}} \delta_{Qa_2}$ | $\frac{1}{\sqrt{3}}[1\,1\,1]^\intercal$ | 8 |
| 3 | $\frac{1}{4}\sum_{Q\in\mathcal{G}} \delta_{Qa_3}$ | $\frac{1}{\sqrt{2}}[1\,0\,1]^\intercal$ | 12 |
| 4 | $\frac{1}{2}\sum_{Q\in\mathcal{G}} \delta_{Qa_4}$ | $(1+\tan^2\frac{\pi}{6})^{-1/2}[1\,0\,\tan\frac{\pi}{6}]^\intercal$ | 24 |
| 5 | $\sum_{Q\in\mathcal{G}} \delta_{Qa_5}$ | $(1+\tan^2\frac{\pi}{12}+\tan^2\frac{\pi}{6})^{-1/2}[1\,\tan\frac{\pi}{12}\,\tan\frac{\pi}{6}]^\intercal$ | 48 |
| 6 | $g_1+g_2+g_3+g_4+g_5$ | | 98 |

Table 1. Grid functions with octahedral symmetry. Each function $g_i$, $1 \leq i \leq 6$, takes the value 1 on its support and is invariant under $\mathcal{G}$.

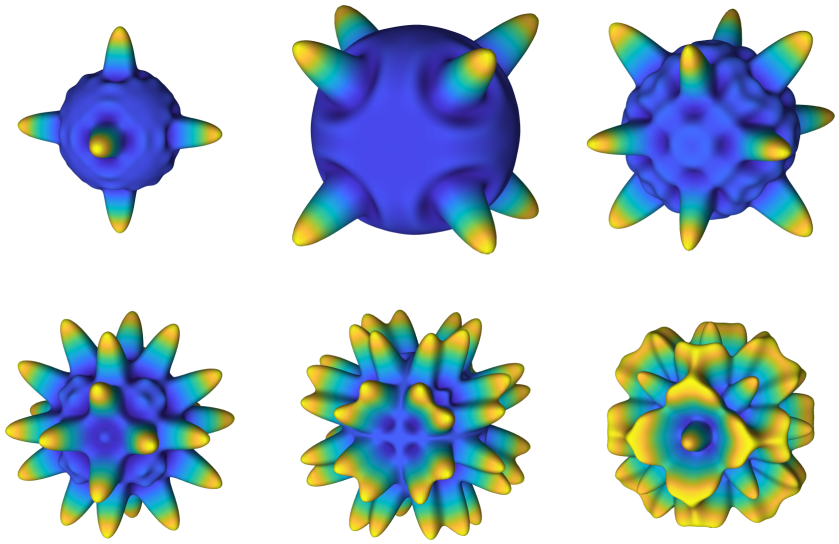

Figure 1. Interpolation with octahedral symmetry. For every $1 \leq i \leq 6$, the symmetric function $\mathcal{I}_N g_i$ is represented by the surface $(1.5 + \mathcal{I}_N g_i(x))x$, $x \in \mathbb{S}^2$.

Second, we assess the invariance of the interpolation space, stated in Theorem 5, and the commutation between interpolation and rotation, stated in Corollary 7.(i). For that purpose, for each basis function $u_j \in \mathcal{U}_N$, we compare $u_j(Q^\intercal \cdot) = [\mathcal{I}_N u_j](Q^\intercal \cdot)$ with $\mathcal{I}_N[u_j(Q^\intercal \cdot)]$. Indeed, by linearity, Corollary 7.(i) is equivalent to:

$$\forall 1 \leq j \leq \bar{N},\ \forall Q \in \mathcal{G},\ [\mathcal{I}_N u_j](Q^\intercal \cdot) = \mathcal{I}_N[u_j(Q^\intercal \cdot)].$$

If this condition is achieved, then for each basis function $u_j$, $u_j(Q^\intercal \cdot) = [\mathcal{I}_N u_j](Q^\intercal \cdot) \in \operatorname{Ran} \mathcal{I}_N = \mathcal{U}_N$, which implies Theorem 5.(iii) by linearity. This also implies Theorem 5.(ii), due to $u_j(Q^\intercal \cdot) \in \mathcal{Y}_n \cap \mathcal{U}_N = \mathcal{V}_n$. We compare the functions on a fine grid $\mathrm{CS}_M$ ($M = 33$), by computing the relative error

$$\epsilon_{N,j}(Q) := \frac{\max_{x \in \mathrm{CS}_M} |u_j(Q^\intercal x) - \mathcal{I}_N[u_j(Q^\intercal \cdot)](x)|}{\max_{x \in \mathrm{CS}_M} |u_j(x)|}.$$

Then we compute the maximal error $\epsilon_N$, and we repeat the procedure for several values of $N$:

$$\epsilon_N := \max\{\epsilon_{N,j}(Q),\, Q \in \mathcal{G},\, 1 \le j \le \bar{N}(N)\}, \quad 1 \le N \le 16. \tag{10}$$

The results reported in Table 2 are in agreement with the invariance stated in Theorem 5 and Corollary 7.(i).

| $N$ | 1 | 2 | 3 | 4 | 5 | 6 | 7 | 8 |
|---|---|---|---|---|---|---|---|---|
| $\epsilon_N$ | 2.5e-15 | 3.4e-15 | 7.8e-15 | 1.4e-14 | 9.7e-15 | 9.3e-15 | 1.3e-14 | 1.1e-14 |
| $N$ | 9 | 10 | 11 | 12 | 13 | 14 | 15 | 16 |
| $\epsilon_N$ | 1.4e-14 | 1.5e-14 | 1.9e-14 | 1.7e-14 | 3.4e-14 | 2.2e-14 | 1.8e-14 | 2.9e-14 |

TABLE 2. Numerical invariance: $u_j(Q^\intercal \cdot) = \mathcal{I}_N[u_j(Q^\intercal \cdot)]$, $Q \in \mathcal{G}$, up to relative error $\epsilon_N$ (10).

6.2. **Quadrature weight.** We have computed the quadrature weight function $\omega_N \in \mathcal{F}(\mathrm{CS}_N)$ for $1 \le N \le 32$, and $N = 64$. Some of them are displayed in Figure 2. As can been observed, the weight appears to be positive, $\omega_N > 0$. The maximum value is reached at the center of a panel. Some statistics of the weights are given in Figure 3. It reveals that the distribution of the weights $\omega_N$ is quasi-uniform. In particular,

$$\frac{\max \omega_N}{\min \omega_N} \approx \sqrt{2}.$$

This coincides with the ratio between the surface element at the center of a panel of $\mathrm{CS}_N$, and the smallest surface element of a panel, (see [17, Eq. (20)]).

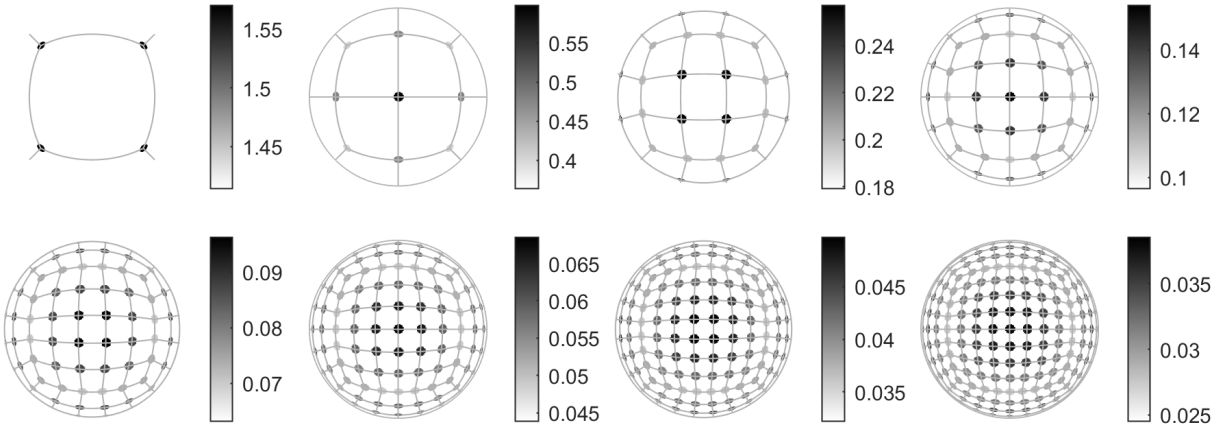


FIGURE 2. Representation of the weight values $\omega_N$, for the eight Cubed Spheres with $1 \le N \le 8$.

6.3. **Quadrature of test functions.** We test the accuracy of the quadrature formula $\mathcal{Q}_N$ on the series of functions reported in Table 3. They are displayed in Figure 4. These functions serve as testing functions for quadrature assessment. References are indicated in Table 3. The exponential function $f_1$ is a smooth, non-trivial function. The Franke function $f_2$ is a standard test case. The function $f_3$ is smooth, except near the South pole, where it has an infinite spike. The cosine cap function $f_4$ is continuous but is not differentiable on the circle $z = \frac{\sqrt{3}}{2}$. The

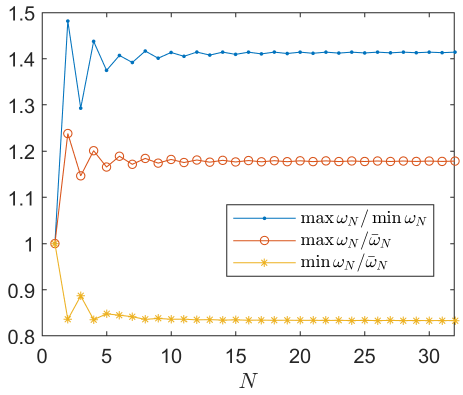


FIGURE 3. Statistical distribution of the weight values $\omega_N$ in (7), $1 \le N \le 32$. The maximum, minimum, and mean values satisfy $\max \omega_N \approx 1.41 \min \omega_N$, $\max \omega_N \approx 1.18\,\bar{\omega}_N$, and $\min \omega_N \approx 0.83\,\bar{\omega}_N$.

| $i$ | $f_i(x,y,z)$ | $\int_{\mathbb{S}^2} f_i(x,y,z)\mathrm{d}\sigma$ | Ref. |
|---|---|---|---|
| 1 | $\exp(x)$ | $14.7680137457653\cdots$ | [3, 11] |
| 2 | $\frac{3}{4}\exp[-\frac{(9x-2)^2}{4} - \frac{(9y-2)^2}{4} - \frac{(9z-2)^2}{4}]$ $+\frac{3}{4}\exp[-\frac{(9x+1)^2}{49} - \frac{9y+1}{10} - \frac{9z+1}{10}]$ $+\frac{1}{2}\exp[-\frac{(9x-7)^2}{4} - \frac{(9y-3)^2}{4} - \frac{(9z-5)^2}{4}]$ $-\frac{1}{5}\exp[-(9x-4)^2 - (9y-7)^2 - (9z-5)^2]$ | $6.6961822200736179523\cdots$ | [2, 4, 7, 12, 16] |
| 3 | $\frac{1}{10}\frac{\exp(x+2y+3z)}{(x^2+y^2+(z+1)^2)^{1/2}}\mathbf{1}(z > -1)$ | $4.090220018862976\cdots$ | [2] |
| 4 | $\cos(3\arccos z)\mathbf{1}(3\arccos z \le \frac{\pi}{2})$ | $\frac{\pi}{8}$ | inspired from [2] |
| 5 | $\mathbf{1}(z \ge \frac{1}{2})$ | $\pi$ | |
| 6 | $\frac{1}{9}[1 + \mathrm{sign}(-9x - 9y + 9z)]$ | $\frac{4\pi}{9}$ | [4, 7, 12, 16] |

TABLE 3. Several test functions and exact mean values.

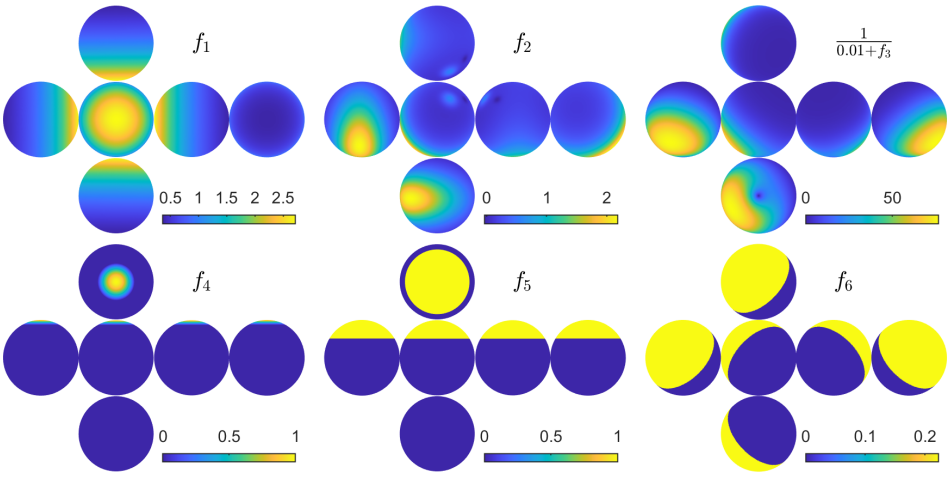


FIGURE 4. Test functions of Table 3.

function $f_5$ is the characteristic function of a spherical cap; it is not continuous. Similarly, the discontinuous function $f_6$ represents a hemisphere; it is a standard test function.

We report in Table 4 the quadrature error

$$\eta_N(f_i) = \left| \int_{\mathbb{S}^2} f_i \mathrm{d}\sigma - \mathcal{Q}_N f_i \right|, \quad N = 1,\ 2,\ 4,\ 8,\ 16,\ 32,\ 64, \quad 1 \le i \le 6.$$

| $N$ | $\bar{N}$ | $\eta_N(f_1)$ | $\eta_N(f_2)$ | $\eta_N(f_3)$ | $\eta_N(f_4)$ | $\eta_N(f_5)$ | $\eta_N(f_6)$ |
|---|---|---|---|---|---|---|---|
| 1 | 8 | 4.8e-02 | 8.2e-01 | 2.4e-01 | 3.9e-01 | 3.1e+00 | 6.7e-16 |
| 2 | 26 | 2.0e-06 | 1.5e-02 | 1.7e-02 | 2.1e-01 | 9.9e-01 | 0.0e+00 |
| 4 | 98 | 1.2e-14 | 2.2e-03 | 7.8e-03 | 2.0e-02 | 6.7e-02 | 2.2e-16 |
| 8 | 386 | 1.8e-15 | 9.0e-06 | 3.8e-03 | 4.8e-03 | 6.4e-02 | 6.7e-16 |
| 16 | 1538 | 7.1e-15 | 5.5e-09 | 1.9e-03 | 3.0e-04 | 1.5e-02 | 6.7e-16 |
| 32 | 6146 | 5.3e-15 | 1.8e-15 | 9.5e-04 | 3.1e-04 | 7.9e-03 | 6.7e-16 |
| 64 | 24578 | 3.6e-15 | 1.8e-15 | 4.8e-04 | 1.9e-07 | 2.6e-03 | 4.4e-16 |

TABLE 4. Quadrature error $\eta_N(f_i) = |\int_{\mathbb{S}^2} f_i \mathrm{d}\sigma - \mathcal{Q}_N f_i|$ for the series of functions in Table 3

| $N$ | $r_N(f_1)$ | $r_N(f_2)$ | $r_N(f_3)$ | $r_N(f_4)$ | $r_N(f_5)$ | $\bar{r}_N(f_1)$ | $\bar{r}_N(f_2)$ | $\bar{r}_N(f_3)$ | $\bar{r}_N(f_4)$ | $\bar{r}_N(f_5)$ |
|---|---|---|---|---|---|---|---|---|---|---|
| 1 | 15 | 5.8 | 3.9 | 0.93 | 1.7 | 15 | 2.8 | 5.4 | 2.5 | -0.0033 |
| 2 | 27 | 2.7 | 1.1 | 3.4 | 3.9 | 26 | 3.3 | 1.1 | 3.3 | 1.8 |
| 4 | 2.8 | 7.9 | 1 | 2.1 | 0.077 | 2.1 | 4.1 | 1 | 1.9 | 1.3 |
| 8 | | 11 | 1 | 4 | 2.1 | | 13 | 1.2 | 2.8 | 1.7 |
| 16 | | 22 | 1 | -0.047 | 0.92 | | 24 | 0.92 | 2.2 | 1.4 |
| 32 | | | 1 | 11 | 1.6 | | | 0.93 | 2.7 | 1.6 |

TABLE 5. Convergence rate $r_N(f_i)$ of the error $\eta_N(f_i)$, and convergence rate $\bar{r}_N(f_i)$ of the average error $\bar{\epsilon}_N(f_i)$, over 1000 random orthogonal transformations of the grid.

Moreover, Table 5 reports a rate of convergence $r_N(f_i)$, defined by the equation

$$\eta_{2N}(f_i) = \frac{\eta_N(f_i)}{2^{r_N(f_i)}}.$$

Note that the computations have been performed with Matlab, in double precision. In particular the machine epsilon is approximately $2.2 \times 10^{-16}$; we do not compute the rate when the relative error is close to this value. For the smooth function $f_1$, the error rapidly reaches a value which is about $10^{-14}$. For the Franke function $f_2$, a thinner grid is required to reach such values, but a very fast convergence is still observed. For the spike function $f_3$, the convergence rate is $r_N(f_3) \approx 1$. For the continuous cap function $f_4$, and the discontinuous one $f_5$, the error slowly decreases at a convergence rate depending on the grid size. For the cap function $f_6$, which is discontinuous and "symmetric" (supported by a hemisphere), the error is close to the machine epsilon, independently of the grid size.

6.4. **Sensitivity to the grid orientation.** Here we consider more closely the accuracy of the rule $\mathcal{Q}_N$: we modify randomly the orientation of the grid, [12, 16]. We compute

$$\epsilon_N(f_i, Q) = \left| \int_{\mathbb{S}^2} f_i \mathrm{d}\sigma - \mathcal{Q}_N f_i(Q^\mathsf{T} \cdot) \right|,$$

where $Q$ browses a set of 1000 randomly selected orthogonal matrices (uniform law in $[0, 2\pi]$ for the Euler angles, and uniform law in $\{-1, 1\}$ for the orientation). The worst error, the average error and their ratio are defined by

$$\varepsilon_N(f_i) = \max_Q \epsilon_N(f_i, Q), \quad \bar{\epsilon}_N(f_i) = \tfrac{1}{1000} \sum_Q \epsilon_N(f_i, Q), \quad \rho_N(f_i) = \frac{\bar{\epsilon}_N(f_i)}{\varepsilon_N(f_i)}.$$

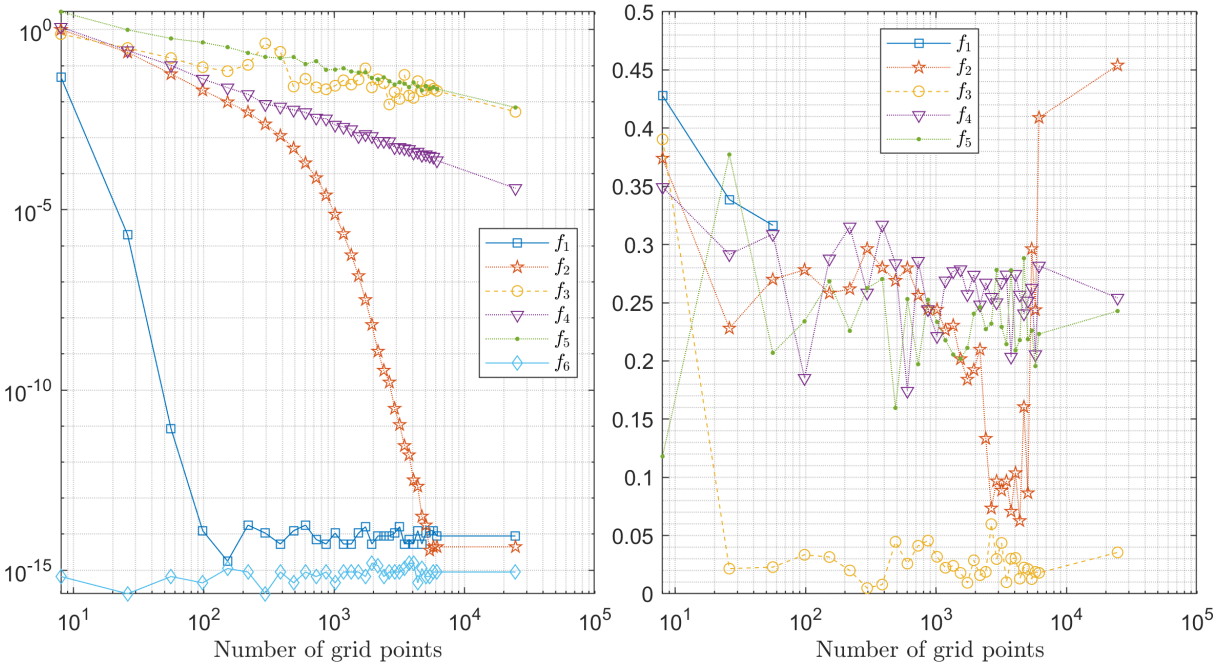


FIGURE 5. Statistics of the quadrature error $\epsilon_N(f_i, Q) = |\int_{\mathbb{S}^2} f_i \mathrm{d}\sigma - \mathcal{Q}_N f_i(Q^\intercal \cdot)|$, where $Q$ scans a set of 1000 random orthogonal matrices. Left: worst error $\varepsilon_N(f_i)$. Right: ratio $\rho_N(f_i) = \bar{\epsilon}_N(f_i)/\varepsilon_N(f_i)$ of the average error divided by the worst one.

The worst error $\varepsilon_N(f_i)$ and the ratio $\rho_N(f_i)$ are displayed[3] in Figure 5. We report in Table 5 a convergence rate $\bar{r}_N(f_i)$ of the average error $\bar{\epsilon}_N(f_i)$, defined by

$$\bar{\epsilon}_{2N}(f_i) = \frac{\bar{\epsilon}_N(f_i)}{2^{\bar{r}_N(f_i)}}.$$

The worst errors $\varepsilon_N(f_1)$ and $\varepsilon_N(f_2)$ rapidly decrease, and $\varepsilon_N(f_6)$ is zero, up to rounding errors. This indicates that the quadrature rule $\mathcal{Q}_N$ efficiently integrates the smooth functions $f_1$, $f_2$, and the symmetric cap function $f_6$, independently of the grid orientation. For the function $f_4$, which is continuous and non-differentiable, the worst error $\varepsilon_N(f_4)$ decreases at constant rate. The decrease of the worst error $\varepsilon_N(f_5)$ of the "generic" cap function $f_5$, which is discontinuous, is slower. And for the spike function $f_3$, the worst error $\varepsilon_N(f_3)$ slowly decreases, with oscillations.

Roughly speaking, Figure 5 indicates that

$$\bar{\epsilon}_N(f_i) \approx 0.25\varepsilon_N(f_i),\ i \neq 3, \quad \bar{\epsilon}_N(f_3) \approx 0.025\varepsilon_N(f_3).$$

Except for $f_3$, the worst error is not very large in comparison with the average error (factor 4). This indicates that the result is almost insensitive to the grid orientation. For the function $f_3$ with a spike, the situation is different (factor 40); the error is sensitive to the grid orientation. Concerning the speed of convergence, we note $\bar{r}_N(f_3) \approx 1$ for the spike function, $\bar{r}_N(f_5) \approx 1.4$ for the discontinuous cap function, $\bar{r}_N(f_4) \approx 2.6$ for the continuous one. The average errors for $f_1$, $f_2$ and $f_6$ rapidly converge, since it was already the case for the worst errors.

6.5. **Comparison with other quadrature rules.** We compare our quadrature rule $\mathcal{Q}_N$ with some spherical quadrature rules of the literature, summarized in Table 6.

**Rules on the Cubed Sphere:** We use two other rules on the Cubed Sphere; CS-BC18 is a correction of some bivariate trapezoidal rule, CS-CP18 is an octahedral rule which

[3]In order to clarify the figure, we have elimated the following ratios: $\rho_N(f_1), N > 3$, and $\rho_N(f_6)$. Indeed, these ratios are "large", because the associated errors are almost zero.

| Abbr. | Description | Ref. |
|---|---|---|
| CS-BBC21 | Interpolation on the Cubed Sphere by spherical harmonics | This article ($\mathcal{Q}_N$) |
| CS-CP18 | Octahedral quadrature on the Cubed Sphere, by least-square | [16] |
| CS-BC18 | Corrected bivariate trapezoidal on the Cubed Sphere | [7] |
| Lebedev | Gauss quadrature, invariant under the octahedral group | [14, 15] |
| t-design | Spherical $t$-design | [19, 20] |

TABLE 6. Quadrature of the literature used for comparison.

minimizes some least-square error concerning the integration of Legendre spherical harmonics.

**Optimal quadrature rules:** We also use "optimal" quadrature rules, whose distribution of nodes is "optimized". Firstly, our rule is invariant under the octahedral group $\mathcal{G}$, so we compare with the Lebedev rule, which is an optimal octahedral rule. Indeed, the optimal grids/weights of the Lebedev rule maximize the degree of precision, with the constraint of invariance under $\mathcal{G}$. Secondly, our weights are quasi-uniform, so we compare with spherical $t$-designs. This rules have equal weights and degree of precision $t$; the associated spherical grids have $\sim \frac{t^2}{2}$ nodes, which is the optimal order.

The results are given on Figure 6. The worst error after 1000 random orthogonal matrices is plotted related to the number of grid points using different quadrature rules.

**Comparison on the Cubed Sphere:** Among the quadrature rules on $\mathrm{CS}_N$, the new rule $\mathcal{Q}_N$ outperforms CS-BC18 for the smooth functions $f_1$ and $f_2$, and for the symmetric cap function $f_6$. The rules $\mathcal{Q}_N$ and CS-CP18 give similar accuracy for most of the cases, with the following exceptions. The rule $\mathcal{Q}_N$ integrates $f_1$ more accurately than CS-CP18 before convergence, and $\mathcal{Q}_N$ converges slightly faster than CS-CP18 for $f_2$.

**Comparison with optimal rules:** For the smooth functions $f_1$ and $f_2$, the rules $\mathcal{Q}_N$ and t-design have similar accuracy, whereas the Lebedev rule converges slightly faster. For the function $f_3$ with a spike, the worst errors are almost similar; they decay slowly with oscillations. For the cap functions $f_4$ and $f_5$, the methods converge slowly with similar accuracy. For the "symmetric" cap function $f_6$, $\mathcal{Q}_N$ and the Lebedev rule are exact (up to rounding errors) and give better accuracy than the t-design rule.

Overall, the rule $\mathcal{Q}_N$ on a fixed grid $\mathrm{CS}_N$ displays remarkable accuracy, compared to "optimal" quadrature methods, which require "optimal" grids (Lebedev and t-design rules).

6.6. **Accuracy of the new quadrature rule.** The quadrature rule $\mathcal{Q}_N$ is designed to integrate exactly any spherical harmonic belonging to the space $\mathcal{U}_N$. In addition, it integrates 15/16 of *all* Legendre spherical harmonics (see Corollary 10). Here, we numerically display detailed accuracy properties of the rule $\mathcal{Q}_N$.

First, for a selected set of tolerances $\epsilon = 10^{-p}$, we give the degree of precision $d_N(\epsilon)$, defined as the largest integer such that

$$\forall |m| \leq n \leq d_N(\epsilon), \left| \int_{\mathbb{S}^2} Y_n^m \mathrm{d}\sigma - \mathcal{Q}_N Y_n^m \right| \leq \epsilon. \tag{11}$$

The results are reported in Table 7. It is observed that except for $N = 3, 4, 64$, the degree $d_N(10^{-14})$ is $2N + 1$ if $N$ is odd, and $2N + 3$ if $N$ is even. For the three exceptions, the degree is found higher than the generic one. We have $d_N(10^{-14}) = 4N - 1$ for $N = 3, 4$, and $d_{64}(10^{-14}) = 2 \cdot 64 + 11$. Furthermore, the Table 7 implicitly displays an accuracy information obtained for some of the Legendre spherical harmonics that are not exactly integrated. For example, in the case $N = 8$, the first error above the threshold $10^{-14}$ belongs to the interval $(10^{-6}, 10^{-4}]$. This error is obtained for the degree $n = 20$ (since the rule is exact for odd degrees).

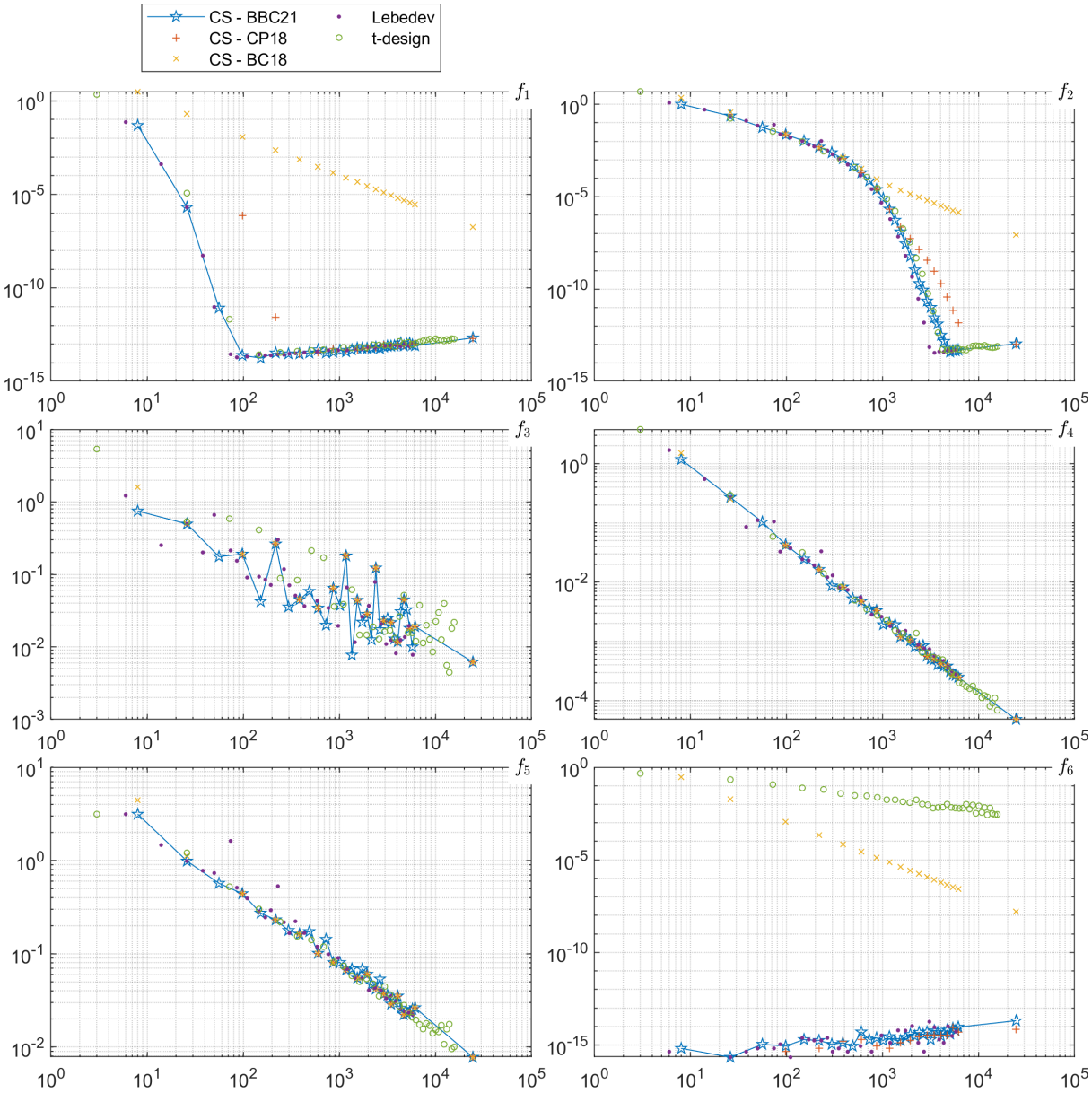


FIGURE 6. Worst quadrature error (for 1000 random orthogonal transformations of the grid), versus the number of grid points.

Second, we focus on the quadrature errors

$$\eta(Y_n^m) = \left| \int_{\mathbb{S}^2} Y_n^m \mathrm{d}\sigma - \mathcal{Q}_N Y_n^m \right|, \quad n \equiv 0\,(2),\ m \geq 0 \text{ and } m \equiv 0\,(4). \tag{12}$$

Here, we consider the series of the 1/16 of all the Legendre spherical harmonics which are possibly non exactly integrated by $\mathcal{Q}_N$, (see Corollary 10). We have computed the quadrature error for this series for $n \leq 1024$, and for the two grids $\mathrm{CS}_N$ with $N = 8$ (386 nodes), and $N = 31$ (5768 nodes). The computed errors are displayed in Figure 7 using both a histogram form, and a cumulative distribution function. As observed, some errors are zero (up to rounding errors). This is consistent with the data in Table 7 (if $n \leq d_N(10^{-14})$, $\eta(Y_n^m) \leq 10^{-14}$). Note also that the largest observed errors belong to the interval $(1, 10)$.

Finally, we further develop these observations by comparing the rule $\mathcal{Q}_N$ with the Lebedev rules. As noted in Remark 11 above, errors with the Lebedev quadrature can occur only with the same set of Legendre functions (referred to as the "1/16 serie"). Therefore, we numerically compare the accuracy of the Lebedev rules with the rule $\mathcal{Q}_N$ on this series. Figure 7 reports a

| $N$ | $\tilde{N}$ | $d_N(10^{-14})$ | $d_N(10^{-12})$ | $d_N(10^{-10})$ | $d_N(10^{-8})$ | $d_N(10^{-6})$ | $d_N(10^{-4})$ |
|---|---|---|---|---|---|---|---|
| 1 | 8 | 3 | 3 | 3 | 3 | 3 | 3 |
| 2 | 26 | 7 | 7 | 7 | 7 | 7 | 7 |
| 3 | 56 | 11 | 11 | 11 | 11 | 11 | 11 |
| 4 | 98 | 15 | 15 | 15 | 15 | 15 | 15 |
| 5 | 152 | 11 | 11 | 11 | 11 | 11 | 11 |
| 6 | 218 | 15 | 15 | 15 | 15 | 15 | 17 |
| 7 | 296 | 15 | 15 | 15 | 15 | 15 | 17 |
| 8 | 386 | 19 | 19 | 19 | 19 | 19 | 21 |
| 9 | 488 | 19 | 19 | 19 | 19 | 19 | 23 |
| 10 | 602 | 23 | 23 | 23 | 23 | 23 | 27 |
| 11 | 728 | 23 | 23 | 23 | 23 | 23 | 27 |
| 12 | 866 | 27 | 27 | 27 | 27 | 29 | 33 |
| 13 | 1016 | 27 | 27 | 27 | 27 | 29 | 33 |
| 14 | 1178 | 31 | 31 | 31 | 31 | 33 | 39 |
| 15 | 1352 | 31 | 31 | 31 | 31 | 33 | 41 |
| 16 | 1538 | 35 | 35 | 35 | 35 | 39 | 45 |
| 17 | 1736 | 35 | 35 | 35 | 35 | 39 | 47 |
| 18 | 1946 | 39 | 39 | 39 | 41 | 43 | 51 |
| 19 | 2168 | 39 | 39 | 39 | 41 | 45 | 55 |
| 20 | 2402 | 43 | 43 | 43 | 45 | 49 | 59 |
| 21 | 2648 | 43 | 43 | 43 | 45 | 49 | 65 |
| 22 | 2906 | 47 | 47 | 47 | 49 | 53 | 65 |
| 23 | 3176 | 47 | 47 | 47 | 51 | 55 | 71 |
| 24 | 3458 | 51 | 51 | 51 | 55 | 59 | 75 |
| 25 | 3752 | 51 | 51 | 51 | 55 | 61 | 79 |
| 26 | 4058 | 55 | 55 | 57 | 59 | 65 | 85 |
| 27 | 4376 | 55 | 55 | 57 | 59 | 65 | 89 |
| 28 | 4706 | 59 | 59 | 61 | 65 | 69 | 95 |
| 29 | 5048 | 59 | 59 | 61 | 65 | 71 | 97 |
| 30 | 5402 | 63 | 63 | 65 | 69 | 75 | 101 |
| 31 | 5768 | 63 | 63 | 65 | 69 | 77 | 105 |
| 32 | 6146 | 67 | 67 | 71 | 73 | 81 | 111 |
| 64 | 24578 | 139 | 143 | 147 | 155 | 183 | 255 |

TABLE 7. Quadrature rule $\mathcal{Q}_N$: observed degree of precision $d_N(\epsilon)$ for various tolerances $\epsilon$. See (11).

comparison between the two Lebedev grids with 434 nodes and 5810 nodes and the cubed sphere rule $\mathcal{Q}_N$ with 386 nodes ($N = 8$) and 5768 nodes ($N = 31$), respectively. It is observed that the Lebedev rules exactly integrate a larger set of spherical harmonics; this was somehow expected, since the Lebedev rules are defined to maximize the degree of precision over octahedral grids. But surprisingly, the distribution of the largest errors of the Lebedev rule is very similar with the one of the rule $\mathcal{Q}_N$. In particular, the largest errors of $\mathcal{Q}_N$, defined on the fixed octahedral grid $\mathrm{CS}_N$, are not above the largest errors of the Lebedev's optimal grid. We even notice on the cumulative density function plots that the number of errors below a moderate tolerance $\epsilon$ can be slightly larger with the rule $\mathcal{Q}_N$; this is observed in particular with $N = 31$ and $\epsilon = 10^{-7}$. These observations indicate the interest of the rule $\mathcal{Q}_N$ when compared with an optimal rule.

## 7. Conclusion

Quadrature on the sphere is important in many respects. It arises in a variety of contexts in physics and chemistry: quantum physics, crystallography, gravimetry, astrophysics, kinetic theory (Boltzmann collision kernel approximations, neutron transport), to quote some of them. Our interest in this question stemmed from numerical experiments with a Cubed Sphere finite difference (FD) solver for the spherical shallow water equations, [8,9]. Important mean quantities must be accurately preserved with time, one of them beeing the mean potential vorticity. Since a FD solver is not conservative by construction, a conservativity analysis must be a posteriori performed, and therefore, an accurate quadrature is needed.

The new rule $\mathcal{Q}_N$ has the property to be quasi-uniform with positive weights. The numerical results can be compared in accuracy with optimal rules such as t-designs and Lebedev rules. This supports the claim of the "approximation power" of the Cubed Sphere. Among the questions open, a better convergence analysis must be performed. Proving the positivity of the weights is also an important goal. This is deferred to a future study. Overall, the symmetry properties of the Cubed Sphere as a support for quadrature seems a promising topic.

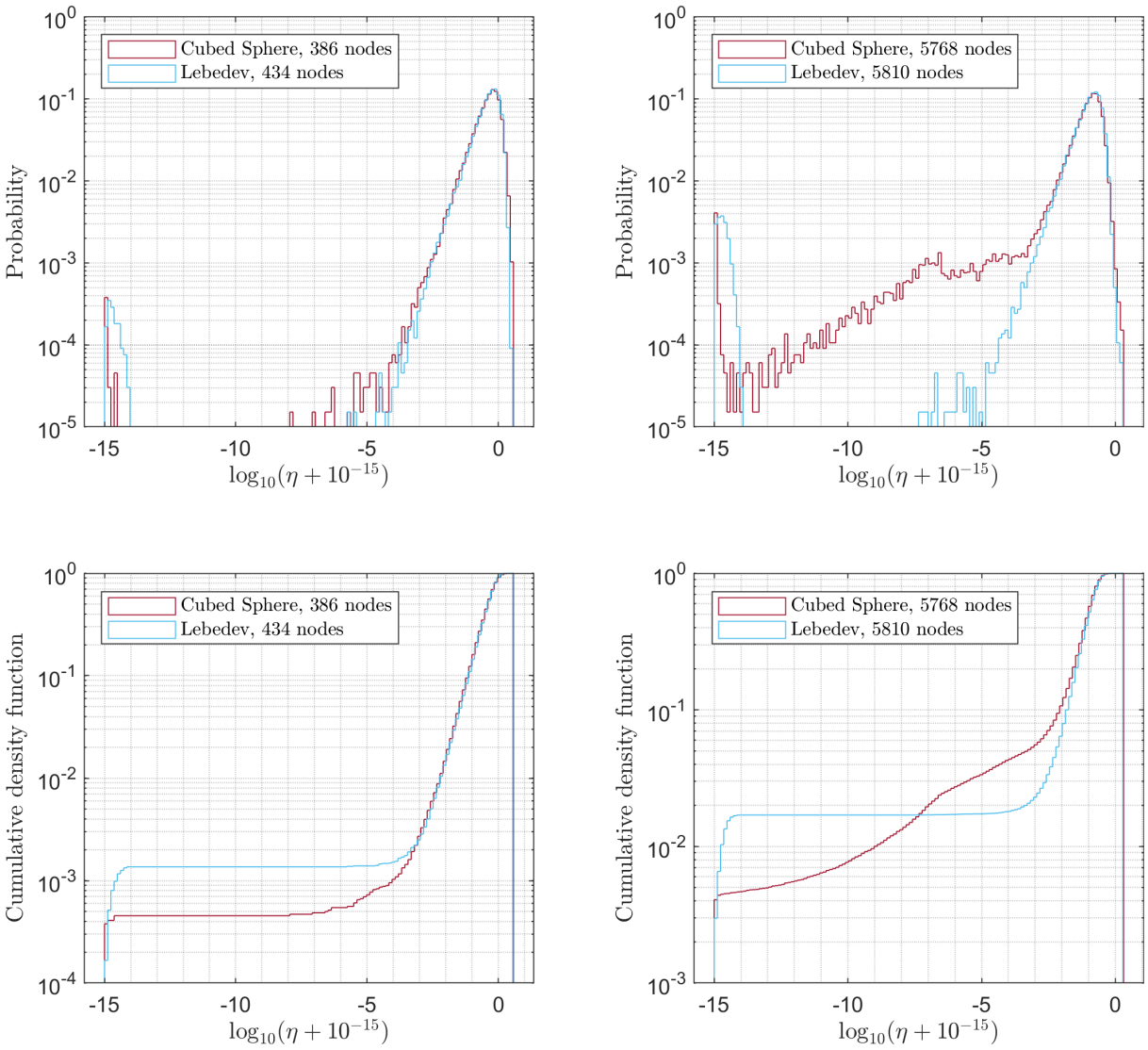


FIGURE 7. Comparison of the errors on the 1/16 series of spherical harmonics (see Corollary 10) between the rule $\mathcal{Q}_N$ and Lebedev's rules for two pairs of grids. Left column: CS (386 nodes)/Lebedev (434 nodes). Right column: CS (5768 nodes)/Lebedev (5810 nodes). The quadrature error $\eta$ is reported for the spherical harmonics $Y_n^m$, with $n \equiv 0\,(2)$, $m \equiv 0\,(4)$, $0 \leq m \leq n \leq 1024$. Top: a histogram with logarithmic rescaling of the errors $\eta$ (12) is displayed for both rules. Bottom: the cumulative density function (cdf) in logarithmic scale for both rules is reported. On these plots, the range of the logarithmic error $\log(\eta+10^{-15})$ has been uniformly divided into 128 classes; for any class $[c_1, c_2)$, the probability (top line) represents the percentage of errors $\eta$ such that $10^{c_1} \leq \eta+10^{-15} < 10^{c_2}$, whereas the cumulative density (bottom line) represents the percentage of errors $\eta$ such that $\eta+10^{-15} < 10^{c_2}$. As a conclusion, the Lebedev's rules exactly integrate more spherical harmonics, but the distributions of the largest errors are similar; moreover, for a large grid, the percentage of errors below a moderate threshold ($\epsilon = 10^{c_2}$) is larger for the rule $\mathcal{Q}_N$ (bottom-right with $\epsilon > 10^{-7}$).

## Appendix A. Quadrature rules data

The data for the various rules used in this study can be found as follows:

- The new rule associated to the Cubed Sphere nodes is available on the open archiv `https://hal.archives-ouvertes.fr/hal-03223150/file/xyzwCSN.zip`
- For the Lebedev rules, we have used the Matlab function `getLebedevSphere` (by R.M. Parrish). The code is available on `https://fr.mathworks.com/matlabcentral/fileexchange/27097-getlebedevsphere`
- The t-designs have been found on R.S. Womersley webpage `https://web.maths.unsw.edu.au/~rsw/Sphere/EffSphDes/sf.html`

## References


[1] C. Ahrens and G. Beylkin. Rotationally invariant quadratures for the sphere. *Proc. Roy. Soc. A: Mathematical, Physical and Engineering Sciences*, 465(2110):3103–3125, 2009.

[2] C. An and S. Chen. Numerical integration over the unit sphere by using spherical t-design. *arXiv:1611.02785v1*, 2016.

[3] K. Atkinson and W. Han. *Spherical harmonics and approximations on the unit sphere: an introduction*, volume 2044. Springer Science & Business Media, 2012.

[4] C. H. Beentjes. Quadrature on a spherical surface. *Technical report, Oxford University - https://cbeentjes.github.io/notes/2015-Quadrature-Sphere*, 2015.

[5] J.-B. Bellet. Symmetry group of the equiangular cubed sphere. *Quat. App. Math.*, 80, 2022.

[6] J.-B. Bellet, M. Brachet, and J.-P. Croisille. Interpolation on the Cubed Sphere with Spherical Harmonics. *https://hal.archives-ouvertes.fr/hal-03202236*, 2021.

[7] M. Brachet. *Schémas compacts hermitiens sur la Sphère: applications en climatologie et océanographie numérique*. PhD thesis, Univ. Lorraine, 2018 (in French).

[8] M. Brachet and J.-P. Croisille. Spherical shallow water simulation by a cubed sphere finite difference solver. *Quat. J. Roy. Met. Soc.*, 147(735):786–800, 2021.

[9] M. Brachet and J.-P. Croisille. A center compact scheme for the shallow water equations on the sphere. *Comp. and Fluids*, (236), 2022.

[10] J. S. Brauchart and P. J. Grabner. Distributing many points on spheres: Minimal energy and designs. *Journal of Complexity*, 31(3):293–326, 2015. Oberwolfach 2013.

[11] J. Fliege and U. Maier. The distribution of points on the sphere and corresponding cubature formulae. *IMA Jour. of Num. Anal.*, 19(2):317–334, 1999.

[12] B. Fornberg and J. M. Martel. On spherical harmonics based numerical quadrature over the surface of a sphere. *Adv. Comp. Math.*, 40(5-6):1169–1184, 2014.

[13] K. Hesse, I. H. Sloan, and R. S. Womersley. Numerical integration on the sphere. In W. Freeden, Z. M. Nashed, and T. Sonar, editors, *Handbook of Geomathematics*. Springer, 2010.

[14] V. I. Lebedev. Quadratures on a sphere. *USSR Comp. Math. and Math. Phys.*, 16(2):10–24, 1976.

[15] V. I. Lebedev and D. Laikov. A quadrature formula for the sphere of the 131st algebraic order of accuracy. *Dokl. Math.*, 59(3):477–481, 1999.

[16] B. Portelenelle and J.-P. Croisille. An efficient quadrature rule on the cubed sphere. *Jour. Comp. App. Math.*, 328:59–74, 2018.

[17] C. Ronchi, R. Iacono, and P. S. Paolucci. The "cubed sphere": a new method for the solution of partial differential equations in spherical geometry. *J. Comp. Phys.*, 124(1):93–114, 1996.

[18] S. L. Sobolev. Cubature formulas on the sphere invariant under finite groups of rotations. *Dokl. Akad. Nauk SSSR*, 146:310–313, 1962.

[19] R. S. Womersley. Spherical designs with close to the minimal number of points. *Applied Mathematics Report AMR09/26, University of New South Wales, Sydney, Australia*, 2009.

[20] R. S. Womersley. Efficient spherical designs with good geometric properties. In *Contemp. Comp. Math. - A celebration of the 80th birthday of Ian Sloan*, pages 1243–1285. Springer, 2018.



† Université de Lorraine, CNRS, IECL, F-57000 Metz, France
*Email address*: `jean-baptiste.bellet@univ-lorraine.fr, jean-pierre.croisille@univ-lorraine.fr`

‡ Université de Poitiers, CNRS, LMA, F-86000 Poitiers, France
*Email address*: `matthieu.brachet@math.univ-poitiers.fr`